Advanced Energy Materials

ADVANCED ENERGY MATERIALS
www.advenergymat.de

PERSPECTIVE OPEN ACCESS

Roadmap for High-Throughput Ceramic Materials Synthesis and Discovery for Batteries

Jesse J. Hinricher[1,2] | Katarzyna P. Sokol[1] | Philipp Simons[1] | Kun Joong Kim[3] | Michael Foshey[4,5] | Yunsheng Tian[4,5] | Thorben Prein[2,3] | Lincoln J. Miara[6] | Elsa Olivetti[1] | Wojciech Matusik[4,5] | Jennifer L. M. Rupp[1,2,3,7]

[1]Department of Materials Science and Engineering, Massachusetts Institute of Technology, Cambridge, Massachusetts, USA | [2]TUMint Energy Research, Garching, Germany | [3]Department of Chemistry, Technical University of Munich, Garching, Germany | [4]Computer Science and Artificial Intelligence Laboratory, Massachusetts Institute of Technology, Cambridge, Massachusetts, USA | [5]Department of Electrical Engineering and Computer Science, Massachusetts Institute of Technology, Cambridge, Massachusetts, USA | [6]Advanced Materials Lab, Samsung Research America, Cambridge, Massachusetts, USA | [7]Fritz-Haber-Institute of the Max-Planck- Society, Berlin, Germany

Correspondence: Jennifer L. M. Rupp (jrupp@tum.de)

Received: 4 November 2025 | **Revised:** 22 January 2026 | **Accepted:** 23 January 2026

Keywords: automated synthesis | battery | Bayesian optimization | machine learning | solid-state electrolyte

ABSTRACT

Global energy demand is projected to grow 30% within the next three decades, driven primarily by population growth and urbanization, leading to greater material needs in energy, and necessitates a new regime of accelerated research via a fundamentally improved strategy. In this perspective, we examine traditional ceramic synthesis methods for high-throughput synthesis and optimization, and highlight requirements and opportunities of synthesis routes for rapid alterations in the future. Such a strategy relies on flexible direct liquid precursor-to-solid film methods rather than traditional, but slower, solid-state methods. Application of computer-aided decision making takes in variables at all levels of fabrication and operates on both material and device characteristics to initialize and optimize the search for higher-performance devices, not just narrow materials optimization. Collectively, we provide a blueprint for accelerated ceramic materials and device improvements of next-generation materials research targeting energy storage.

1 | Introduction

The projected 34% global energy demand rise over the next 30 years [1] requires an increase in renewables to replace fossil fuels and reduce carbon footprints in energy supply and material manufacture. Considering green energy supply solutions, electrochemical energy storage is one option to buffer the intermittent solar and wind supply. In particular, lithium-ion batteries (LIBs) have shown remarkable promise to store energy due to performance largely driven by material discoveries and cell integration. With deeper electric vehicle market penetration and consumer demand, larger energy density and fast charging are areas of active research, but are limited to improve beyond the projected 489 Wh kg^{-1} energy density by 2030 by the carbon graphite anode capacity (372 mA h g^{-1} [2]) [3]. In the face of growing climate change, society must orient research and development efforts to improving energy storage beyond these limitations. Here, by exchanging a classic LIB polymer separator with a solid-state lithium-conducting electrolyte [4–6] allows for hybrid and solid-state batteries to replace classic anodes with pure lithium metal anodes (3860 mA h g^{-1}), thereby improving energy density by 30% (~1000 Wh L^{-1} compared to 770 Wh L^{-1} [7, 8]). The scope of this perspective is limited to lithium-conducting electrolytes, but

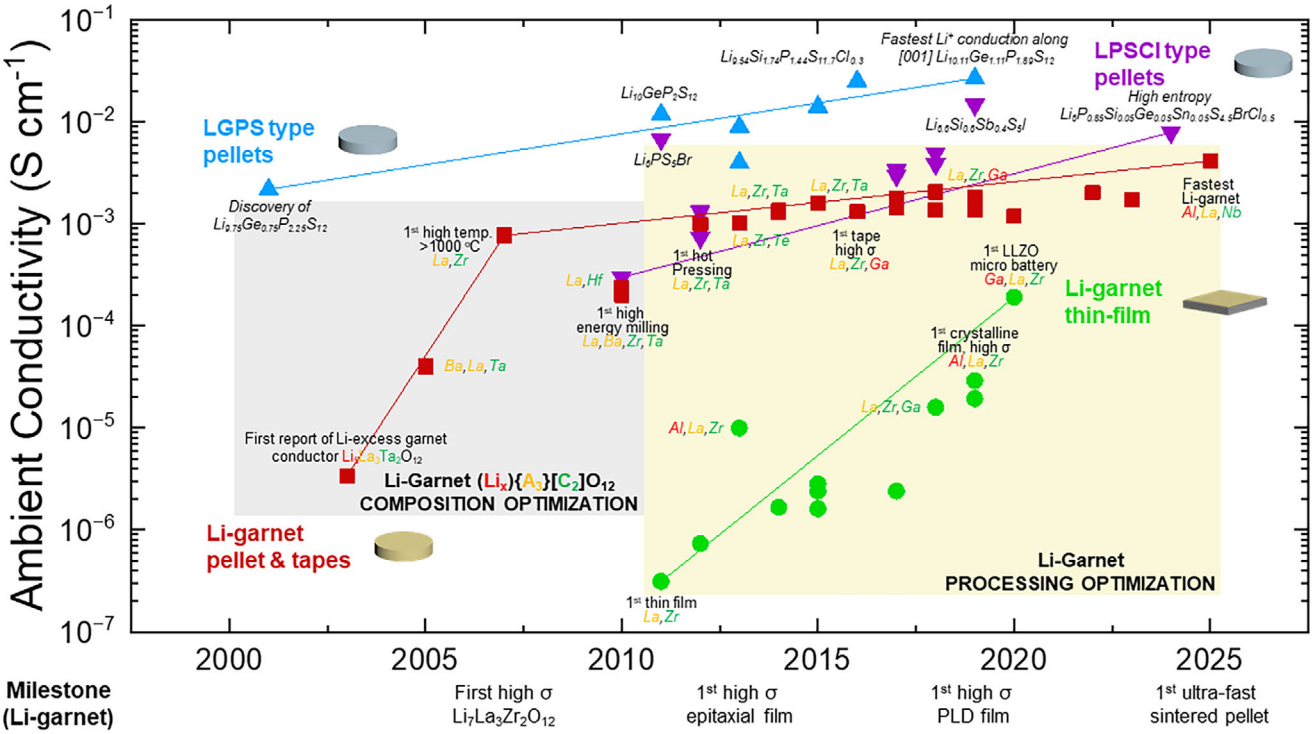

FIGURE 1 | Historical development of selected solid electrolyte conductivities of lithium garnets ($Li_7La_3Zr_2O_{12}$) and sulfides ($Li_{10}GeP_2S_{12}$, Li_6PS_5Cl). Advancements in conductivity for Li-garnets (pellets and tapes: red squares; films: green circles) were achieved first by dopant optimization and then by processing optimizations. $Li_{10}GeP_2S_{12}$ (blue upward-facing triangles) shows substantially higher conductivity, improved by compositional optimization, but suffers from low chemical stability. Li_6PS_5Cl (purple downward-facing triangles) exhibits moderate conductivity similar to Li-garnet pellets and tapes. Overall, it has taken several years of time and capital investment from the first prediction, discovery, and conductivity optimization to thin-film processing of the reported electrolytes. References can be found in the Supporting Information S1. σ, conductivity.

beyond-lithium technology can benefit from similar approaches and strategies.

Traditional experimental strategies adjust material parameters designed to lead to structure outcomes that result in materials properties that in turn give rise to improved device-level performance. Figure 1 displays the ambient-temperature conductivity over time for selected established solid electrolytes for next generation batteries, including the oxide Li-garnet ($Li_7La_3Zr_2O_{12}$), sulfide material classes represented by $Li_{10}GeP_2S_{12}$ (LGPS), and Li_6PS_5Cl (LPSCl). The oxide Li-garnet is a particularly interesting case study demonstrating the long path to achieving high conductivity. Bulk LLZO studies from 2003-2011 mainly focused on compositional optimization of the bulk, while a few works reported both compositional and process tuning (e.g., first high temperature sintering >1000°C [9], first high energy milling [10], first sol-gel synthesis [11]). From 2012 until now, processing optimization of bulk and thin-film fabrication has been the main focus with most studies selecting the $Li_7La_3Zr_2O_{12}$ composition due to its high ionic conductivity. High conductivities (>1 mS cm^{-1} at ambient) can be achieved by appropriate dopant choice and high relative density. Solution-based synthesis (e.g., sol-gel based), high temperature sintering >1000°C, high energy milling, hot-pressing, or a combination of these can improve the relative density and therefore increase total conductivity. It is important to note that both optimized composition and processing (high density) are required for high total conductivity.

Development has progressed in a slow manner, as shown in Figure 1—either manually or autonomously—with few deviations until now. Typically, the metrics of each step depend only on the parameters of the preceding step, and rarely are earlier variables are considered with respect to device performance. This is an inherent problem in the solid-state electrolyte research community and the field should adapt to using large data models and high-throughput synthesis to more quickly advance electrochemical device performance. Figure 2a,b shows that the field of solid-state electrolytes and cathodes lacks the ability to make films in the thickness range of approximately 1–10 μm and there is still room to explore using rapid synthesis methods such as those described herein.

Automation paradigms that have been successfully used in battery research include: (i) combinatorial synthesis and high-throughput screening densified electrolyte [12] and cathode [13] films using X-ray diffraction, (ii) computational simulations of battery component stability [14–18], and (iii) data mining on Li-ceramic manufacture and solidification parameters [19], (iv) machine learning (ML) analysis and prediction of Raman, phonon, and electrochemical impedance spectra [20, 21], and cell performance prediction [22–24]. More recently, an autonomous lab was used to synthesize 41 novel materials via solid-state processing methods [25]. Overall, ML-guided routes combined with automation can overcome existing bottlenecks in solid-state synthesis and mechanisms exploration. In this perspective article, we focus on examining the options and *suitability of altering*

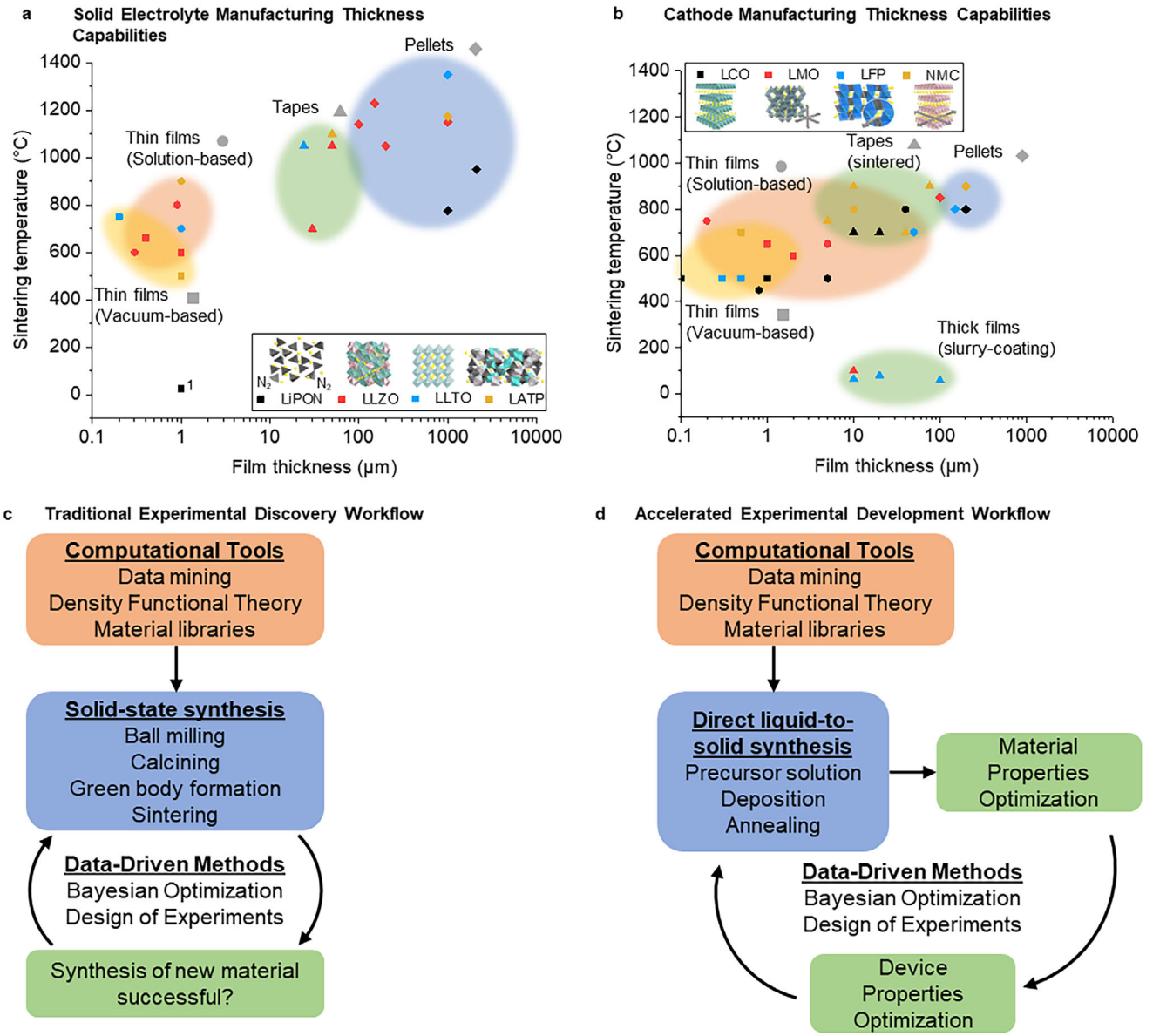

FIGURE 2 | Selected examples of key SSB manufacturing methods and techniques and their automation potential. (a) Selected examples of ceramic manufacturing of solid electrolytes for SSBs and their automation potential. LiPON (vacuum-based thin films, solid-state synthesized pellets), LLZO (vacuum-based thin films, solution-based thin films, tapes, and pellets), LLTO (vacuum-based thin films, solution-based thin films, tapes, and pellets), and LATP (vacuum-based thin films, solution-based thin films, tapes, and pellets). (b) Selected examples of ceramic manufacturing of solid cathodes for SSBs and their automation potential. LCO (vacuum-based thin films, solution-based thin films, tapes, and pellets), LMO (vacuum-based thin films, solution-based thin films, tapes, and pellets), LFP (vacuum-based thin films, solution-based thin films, tapes, and pellets), and NMC (vacuum-based thin films, solution-based thin films, tapes, and pellets). The 'unsintered' tapes have been fabricated using commercially purchased and previously sintered powders, and not subjected to the post-deposition sintering step after tape-casting. (c) Traditional autonomous experimental strategy showing that solid-state synthesis is heavily relied on to synthesize new materials. d, Proposed new experimental strategy using wet-chemical synthesis to optimize both material and device characteristics. Abbreviations: SSB, solid-state battery; LiPON, $Li_xPO_yN_z$; LLZO, $Li_7La_3Zr_2O_{12}$; LLTO, $Li_xLa_yTiO_3$; LATP, $Li(Al,Ti)_2(PO_4)_3$; LCO, $LiCoO_2$; LMO, $LiMn_2O_4$; LFP, $LiFePO_4$; NMC, $Li(Ni,Mn,Co)O_2$.

the ceramic synthesis routes themselves for high throughput and guided by ML. For instance, while autonomous high-throughput synthesis can be promising for materials discovery, as seen in Figure 2c, it often relies on solid-state synthesis for simplicity and ability to incorporate a wide set of cations, but is fundamentally expensive [26] and time consuming, necessitating examining other methods. Furthermore, the integration of the solid components into a battery remains indirect, as additional steps in interface engineering and co-assembly of electrolytes with electrodes remain and require attention. On the contrary, as shown in Figure 2d, faster ceramic synthetic methods using direct liquid precursor-to-solid film routes impart such a fundamental boost, that a wide range of compositions can be quickly synthesized, but often stoichiometries are more challenging to control. The liquid precursor approach is less expensive and often comes with the added benefit that device-level characteristics can be accounted

for. Increasing the speed of synthesis improves the experimental pipeline only to a point; coupling fast synthesis to efficient characterization allows more rapid information gathering while streamlining data collection. In brief, depending on the ceramic synthesis route selected for high throughput, one may either opt for tight stoichiometry control but at high cost and low screening speed, or for looser stoichiometry control at lower costs and rapid screening.

In this perspective, we propose a framework of considerations to accelerate research and development of solid-state electrolytes based on computationally determined initial compositions, high-throughput synthesis methods, and increasing characterization complexity, all combined with computer-aided decision making design of experiments (DoE) or Bayesian optimization ML approach [27, 28]. To date, ceramicists generally do not adequately appreciate that solid-state synthesis routes are too slow to rapidly tailor solid-state chemistry and densification protocols. In this work, we highlight that direct liquid precursor-to-solid film methods have disruptive potential for direct dense film deposition to iterate quickly while avoiding classic sintering. Such methods have untapped potential for automation due to low cost, easy scale-up, simple equipment, and adaptable experimental protocol. Then, we assess chemical and structural characterization techniques applicable to both materials and devices in terms of data collection efficiency. This analysis and framework will accelerate solid-state electrolyte developments and decrease the time between new materials discoveries and device performance optimization.

2 | High-Throughput Development of Ceramics

2.1 | Optimizing Ceramic Materials

By using a hierarchical approach, as demonstrated by the funnel in Figure 3, fundamentally faster and more affordable methods are applied early in an experimental campaign, and more elaborate and expensive techniques are reserved for the most promising candidates later in the synthetic pipeline. By starting with computationally determined initial compositions (above the funnel in Figure 3a), researchers can choose a reasonable starting point for their optimization of materials or the discovery of new ones. Automated characterization guided by ML data analysis will accelerate the speed of data processing and increase the standardization of data analysis. Characterization techniques can be divided into two categories: in-situ processing validation and ex-situ structural/chemical characterization, as shown in Figure 3a. In situ methods monitor the deposition and formation process of ceramics, using high-speed cameras, optical photography, and optical microscopy and verify that the synthesized ceramics are dense to a first-order approximation. High-speed cameras can analyze droplet radii during spray pyrolysis or ink-jet printing. Optical imaging and microscopy would analyze film morphology by detecting cracks, color variations, and other characteristic features of the deposition process. These monitoring techniques can be automated by implementing rather mature image recognition algorithms. Shown in Figure 3b, ex-situ structural and chemical characterization tools such as Raman spectroscopy, scanning electron microscopy, inductively coupled plasma spectroscopy, and x-ray diffraction can analyze the crystallographic structure and phase, microstructure, atomic composition, and near-order vibrational arrangement. The goal of this characterization is to assess key parameters that govern the behavior of solid-state electrolytes, such as the degree of lithiation, degree of crystallinity, crystal structure, dopant level, and electronic structure. Raman and Fourier-transform infrared (FTIR) spectroscopy probe the chemical structure and phases of materials [29]. Both techniques can be easily automated and do not require complex periphery equipment such as high-vacuum chambers. Currently, spectra of new structures are relatively expensive to compute and spectral databases are limited, making the automated interpretation challenging [30]. However ML has been used to recognize and analyze Raman spectra of Li-ion battery electrodes [20] and for material identification in general [31]. Raman spectroscopy is particularly adept at distinguishing different ceramic phases in cases where x-ray diffraction (XRD) cannot [32]. Shown in Figure 3c, the synthesized material can be analyzed relative to calculated phonon spectra from Density Functional Theory or molecular dynamics, and simple metrics can be employed to compare them [33].

2.2 | Optimizing Devices

Once the material has been optimized, there is also the opportunity to increase the degree of complexity by incorporating optimized materials into half or full electrochemical devices, like a battery or fuel cell. Furthermore, an even higher degree of complexity can be achieved by fabricating a multilayer structure by performing sequential depositions on the substrate, that is, first deposit the cathode layer, then the solid-state electrolyte layer, then the anode layer. Additionally, each layer can be optimized independently to achieve optimal density and phase, but also the entire device stack can be optimized for the lowest interfacial resistance. A high interfacial resistance typically originates from a resistive interphase formed due to chemical mixing during processing, for example, densification at elevated temperature, see examples between layered cathodes (LCO [34], NMCs [35]) and oxide electrolytes (LLZO). To mitigate such incompatibilities, thin interlayer coatings (for example, $LiNbO_3$, $LiTaO_3$, Li_2ZrO_3) can be introduced to block cation interdiffusion and maintain chemical potential balance at oxide–oxide interfaces [36]. Alternatively, compositional grading via co-deposition or sequential decomposition synthesis can smooth interfacial reactivity and reduce the formation of resistive interphases. Likewise, processing conditions can be optimized for chemical compatibility and microstructure at the interfaces. Electrochemical impedance spectroscopy is typically used to detect any changes in chemical composition and microstructure within sprayed cathode and electrolyte bi-layer stacks and optimize the deposition conditions of independent layers to achieve a low stack resistance or areal specific resistance (ASR). For example, numerous half-cells can be tested and filtered based on the target ASR of $<40\ \Omega\ cm^2$ [37]. Optimizing the entire device stack, including the interface, could improve desired properties such as increasing resistance to Li dendrite penetration and critical current density, given that synthesis parameters can be adjusted to achieve the best *device* performance, rather than simply the best *layer* performance. Once the materials of a full multi-layered device are optimized in terms of the chemical composition and structure, device-level performance optimization can be conducted.

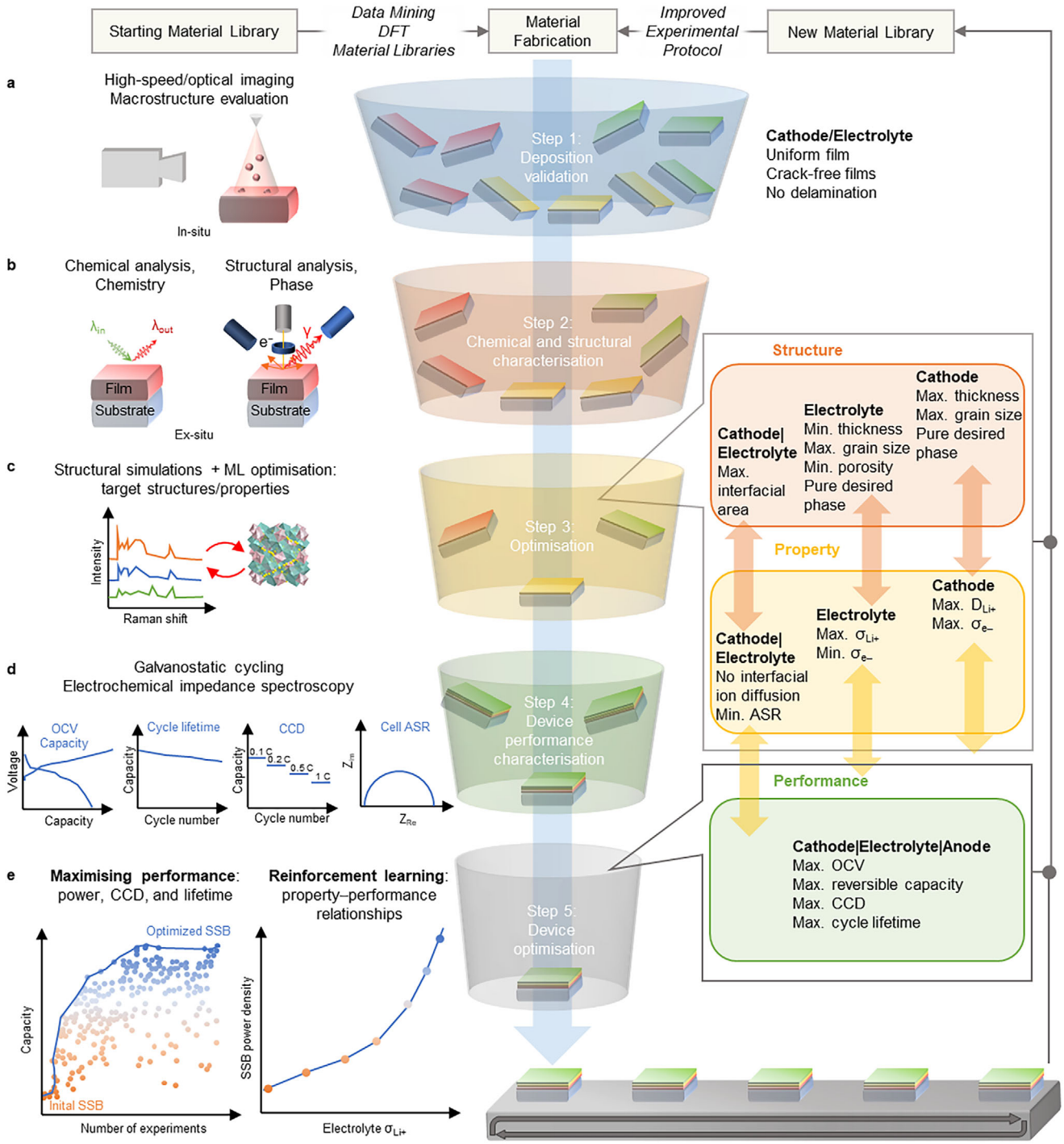

FIGURE 3 | Optimization protocol for structural and electrochemical performance characterization of SSBs. Characterization and optimization stages: (a) optical validation of process, (b) chemical and structural characterization, and (c) ML-driven optimization and reinforcement learning of structure-property relationships. Structure optimization involves obtaining pure desired material phase, maximizing grain size, minimizing thickness and porosity of solid electrolyte, and maximizing the electrolyte|cathode contact area. Property optimization involves minimizing interfacial ion diffusion and area-specific resistance (ASR), maximizing Li^+ conduction/diffusion, while minimizing/maximizing e^- conductivity of an electrolyte/cathode, respectively. (d) SSB performance characterization based on galvanostatic cycling and electrochemical impedance spectroscopy. Key electrochemical performance metrics include open-circuit voltage (OCV), critical current density (CCD), reversible capacity, cycling lifetime, and the cell's ASR. (e) ML-driven optimization, based on active learning (optimal experimental design) of performance parameters and reinforcement learning of property-performance relationships. Full SSB optimization involves maximization of OCV, reversible capacity, CCD, cycle life, and minimization of cell's ASR. Abbreviations: DFT, density functional theory; ML, machine learning; OCV, open-circuit voltage; CCD, critical current density; ASR, area-specific resistance; SSB, solid-state battery; σ_{Li+}, Li^+ ion conductivity; σ_{e-}; electronic conductivity; D_{Li+}, Li+ diffusion coefficient.

Device-specific electrochemical properties can also be optimized. These include, in the case of batteries, critical current density [38], area-specific resistance, coulombic efficiency, and capacity retention [24], but other electrochemical parameters can also be applied to fuel cells, capacitors, or other devices. Collecting and analyzing these parameters is easy to automate, but can be time-consuming to collect (e.g., device lifetime can take weeks or months to determine), and so are better left for later in the analytical pipeline, as indicated by their inclusion at the narrower end of the funnel shown in Figure 3d.

Examples of device-level parameter optimization are chosen from the battery field. The first electrochemical device characterization is typically a measurement of the open-circuit voltage (OCV), used to predict device lifetime and state of charge [39–42]. Algorithms have been used to predict device lifetime by analyzing efficiency using initial cycling performance [23, 41, 43–46]. ML algorithms can minimize critical current density, minimize area-specific resistance, increase capacity retention [24], and maximize coulombic efficiency by tuning device parameters. These various metrics can be combined (Figure 3e) to give an overall impression of total device performance. One effective method to evaluate aggregate performance is to calculate a Pareto front that accounts for trade-offs between multiple, often conflicting, objectives [47]. The output of such an optimization is a Pareto set of solutions that give rise to the optimum performance of, in this case, electrochemical devices.

We will now explore each of the separate aspects of ceramic materials and device optimization using Figure 3 as a guide. While computational efforts include data mining, density functional theory, and material libraries, we select data mining to explore further in the next section.

3 | Enhancing Optimization Loops Through Data-Guided Methods

3.1 | Inverse Materials Design and Optimization

In general, two complementary approaches can be distinguished for data-driven materials optimization. First, one can directly optimize a target property, for example, by maximizing ionic conductivity in a solid-state battery electrolyte. Second, one can pursue the experimental realization of a computationally predicted candidate material, for example, a phase identified from DFT-based databases such as the Materials Project [48], followed by iterative refinement of synthesis conditions and structure to converge toward the predicted compound. The former is guided primarily by the measured performance metric, whereas the latter is guided by agreement with a target structure and its associated properties.

3.2 | Efficient Sample Space Exploration

Since both approaches require an optimization strategy to guide the process, they rely on similar methods to guide the experimental optimization. Rather than randomly sampling the design space, established design-of-experiments (DoE) methods [49] provide more principled sampling strategies, such as factorial and space-filling designs, to efficiently explore the design space and identify optimal regions. However, the major drawback of such approaches is that the sampling pattern is determined beforehand and will be fixed throughout the experiments. An attractive alternative is to use Bayesian optimization (BO), an adaptive sampling strategy that proposes new experiments based on prior evaluations, enabling efficient exploration of the campaign's design space [50, 51]. Thereby, BO iteratively fits a probabilistic surrogate model to the measured objective and uses an acquisition function to select the next experiment by trading off exploration of uncertain regions against exploitation of promising conditions. For a more detailed discussion of BO, please refer to Ref. [52].

Recently, BO has been widely used for the experimental design of different applications that involve physical products and processes, because of its high sample efficiency in exploring the design space and discovering promising solutions. Erps et al. [53] used BO to accelerate the discovery of 3D printing polymers with optimal mechanical properties. BO is also gaining traction in the battery community. For example, Attia et al. [46] used BO to predict battery cell lifetime based on early cycle performance and developed several charging protocols that assessed batteries in just 16 days rather than the typical 500 days. Dave et al. [54] used BO and an automated mixing apparatus to maximize 251 aqueous electrolytes' conductivity and stability window for large-scale energy storage. Complementary to BO, literature-mining and literature-informed models can support campaign initialization by proposing plausible starting points and by constraining the search space using prior reported knowledge.

3.3 | Literature Informed Models

Using BO loops for broad searches of chemical or process design space displays a challenge due to temporal and cost constraints stemming from real-world experimental necessities, as well as the optimizer's inherent limitations [55]. This implies the inevitability of constraining the search space investigated during BO a priori to the experiments. Commonly, this narrowing is done by human researchers, pointing to a smaller subregion of the larger unconstrained materials space [56, 57]. Literature-informed machine learning models can assist within this preliminary stage and help researchers to select subspaces of promising experimental conditions such as promising compositional candidates or synthesis routes, thereby potentially accelerating BO convergence and increasing sample efficiency [58, 59]. They can further be augmented by DFT calculations regarding viable candidates and materials properties [48]. By literature-informed models, we refer to machine learning approaches, such as tree-based methods and deep neural networks, that learn material-specific synthesis conditions or properties from large-scale databases [58–63]. Once trained, these models can propose suitable precursors and synthesis conditions or compositional regions for a given target material or desired property. One area where this approach has gained momentum is the development of synthesis databases, compiled in part through community-driven curation and in part via systematic extraction using automated natural language processing tools [19, 59–61]. These databases span across synthesis reaction types

and diverse material systems, listing processing steps, as well as conditions, such as temperatures and sintering times [64]. Training machine learning models on these datasets enables them to uncover synthesis–structure regularities that inform key decisions, such as precursor selection [58, 65, 66].

We therefore envision a sample-space exploration strategy that combines experimental feedback from the laboratory with prior knowledge extracted from published synthesis and characterization reports. Literature-informed models augment BO surrogates, which are initialized without prior knowledge, by leveraging large, heterogeneous datasets spanning diverse material systems. However, literature-trained models on the other hand face persistent challenges related to data sparsity, reporting bias, and noise [58]. Published procedures often reuse a narrow set of conditions, leaving other regions underrepresented, and unsuccessful experiments are rarely reported, which skews training data toward positive outcomes. Moreover, variation in experimental setups and environmental conditions across laboratories introduces substantial noise, leading to higher predictive uncertainty when models are transferred to a new domain. In contrast, BO can actively probe a constrained parameter space and adapt proposals to a specific laboratory's conditions through iterative experimentation [56]. Thus, literature-informed models are particularly valuable for transferring costly prior knowledge to new problems, while BO provides a mechanism to refine conditions in situ, albeit within a more limited search space [58, 67].

Below we briefly summarize common tasks and representative recent approaches enabled by using literature-mined datasets. Recent studies demonstrate that predicting synthesis properties from literature-derived data is feasible when datasets contain tens of thousands of entries spanning a broad materials space [19, 59, 62, 64]. Current databases encompass rich information, spanning from the ceramic synthesis route employed (e.g., solution, sol-gel, or solid-state), to experimental parameter exploration and exploitation, such as the chemical precursors and specific processing actions [58–62]. These include mixing, sintering, or drying, complemented by parameters such as duration and temperature for each respective step. Thanks to recent advancements in Natural Language Processing, datasets are expected to soon offer even richer contextual details being extracted from experimental publications, including multiple measured properties and in-depth methodological specifics [68, 69]. This will facilitate analyses at a larger scale, paving the way for even more comprehensive investigations. Models displayed in current research are employed for tasks like synthesis method recommendations, process parameter suggestions, and precursor recommendations [19, 59, 62, 64]. In the process parameter suggestion category, the model is given precursor and target compounds and asked to predict suitable process parameters (e.g., sintering temperature and time) [62]. While previous research primarily focused on predicting specific discrete process parameter values, the recent study by Karpovich et al. employs generative model-based methods, that consider the non-uniqueness of process parameters by outputting a distribution of feasible process parameters [58, 70]. Non-uniqueness is exemplified by the fact that a range of calcination temperatures might achieve a successful synthesis reaction, rather than a single specific calcining temperature. The researchers achieved this by modelling solid-state reaction heating steps' process parameter distributions using conditional variational autoencoders (CVAE) [71]. Another task of recent research interest is the suggestion of precursors. Kim et al. constructed a dataset of about 51 000 synthesis actions, training a CVAE predicting precursors for target materials unseen during training [60]. By excluding the most recent publications, they demonstrate that their approach effectively models feasible precursors.

Looking ahead, Bayesian optimization guided by laboratory feedback and complemented by first-principles and literature-informed approaches offers a promising route for accelerating materials optimization. Particularly, employing them in a staged combination might offer a more informed approach for the definition of BO campaign boundaries. This, in turn, can enhance sample efficiencies, resulting in fewer experiments needed to achieve the desired synthesis outcome.

4 | Suitability of Ceramic Manufacturing Methods for High-Throughput Synthesis

Continuing down the funnel of Figure 3, fundamentally faster manufacturing methods are examined as alternatives to traditional ceramic processing in high-throughput research. First, however, these traditional synthesis methods for ceramics are themselves introduced, see [5] for more details. In brief, the example of Li-oxide ceramic synthesis is illustrative and encompasses powder synthesis followed by densification: (i) ball milling metallic salts, (ii) compacting by hydraulic press, and (iii) calcining (700–1000°C) under a specific atmosphere to yield the desired product phase; (iv) if a dense body is desired, a sintering step is added (>1000°C) to form a ceramic pellet or tape. The many transfer steps, pressing, and relatively long times at each step obviate traditional solid-state methods for high-throughput ceramic processing, even if they can be automated. An ideal synthesis technique for ceramic high throughput allows control over the resulting product by changing chemistry, phase and structure via synthesis parameters and creates solid bodies or controlled nanostructures. Ideally, these can be directly transferred as functional building blocks into devices. Vitally, it has high feature precision, and favorable throughput parameters like scalability, low cost, easy role-to-role integration, and short processing time. Such techniques are discussed in this chapter.

Alternatives to solid-state synthesis are shown in Table 1 and are analyzed for their automation potential, requirement for sintering, and ease of film integration into electrochemical devices. Wet chemical techniques have the highest throughput potential because they easily accommodate a wide range of dopants (e.g., cations for Li-based metal oxides) and use a direct "one-step" dense film deposition, evidenced by the example of sequential decomposition synthesis [72] that bypasses the time-consuming powder-to-pellet synthesis. Vacuum-based techniques have the lowest throughput potential because they typically require batch synthesis and have long synthesis times, as well as requiring expensive specialized equipment. Some vacuum methods, like pulsed laser deposition, even require pellet targets—fabricated using solid-state synthesis—before thin films can be synthesized [73]. Combinatorial PLD however can be useful for screening material libraries and often uses multiple targets to alter

TABLE 1 | Summary of Li-ceramic synthesis methods and their potential use in high-throughput synthesis.

Processing technique	Example methods	Advantages for high throughput	Disadvantages of high throughput	Strategy to control lithiation and dopants	Sintering required?
Thin Films (direct liquid-to-solid ceramic synthesis methods)	• Sol gel • Spray pyrolysis • Dip coating • Spin coating	• Easy to control lithiation • Compensate for lithium loss • Easy to control doping amounts • Easy to adjust many different dopants	• Chemically compatible solvents and metal salts needed • Low control of film roughness • Many parameters that control film quality, for example, deposition temperature, rate of droplet incidence on substrate	• Simply overlithiate precu rsor solutions • Dissolve new dopants into precursor solutions	See Figure 4
Calendaring	• Fabrication of sulfide solid-state electrolytes	• No sintering might be required to densify the electrolyte	• The electrolyte must be soft for it to compact under pressure and not fracture	• Overlithiate precursor powders • Add new dopants to precursor mixture	No
Tapes	• Tape casting	• Simple mechanical moving parts • Easy to add new components to slurry	• Time and labor intensive • Precursor salts and slurry solvents must be compatible • Many processing steps: mixing, doctor blading, drying, sintering	• Overlithiate slurry • Add new dopants to slurry	Yes
Pellets (classical sintering)	• Solid-state fabrication	• Easy to incorporate new dopants	• Time and labor intensive • High-temperature sintering (>1000°C) required • Sometimes difficult to achieve high density with new dopants	• Mix in more lithium salts with precursor salts • Add new dopants to precursor mixture	Yes
Pellets (rapid sintering)	• Rapid sintering	• Low lithium loss during sintering	• Extremely high temperat ures required (>1300°C)	• Mix in more lithium salts with precursor salts • Add new dopants to precursor mixture	Yes

(Continues)

TABLE 1 | (Continued)

Processing technique	Example methods	Advantages for high throughput	Disadvantages of high throughput	Strategy to control lithiation and dopants	Sintering required?
Pellets (cold sintering)	• Cold sintering • Spark plasma sintering	• Low temperatures required • Low lithium loss during sintering	• High pressures required for compaction (>400 MPa) • Solvent compatibility with ceramic powder	• Mix in more lithium salts with precursor salts • Add new dopants to precursor mixture	Yes
Thin Films (Vacuum-based)	• Sputtering • PLD	• Rapid adjustment using two targets • High control of film thickness and surface roughness	• Vacuum chamber required and high cost • Difficult to prevent lithium loss during deposition	• Overlithiate target pellet • Add new dopants to new target pellet, only rapidly achievable for two-component films	No

composition as a function of location [74], but integration into electrochemical devices is challenging.

Clearly, direct liquid precursor-to-solid film wet-chemistry techniques, such as sequential decomposition synthesis (SDS), dip-coating, spin-coating, and inkjet printing, have the highest potential for automated rapid SSB oxide material fabrication due to low cost, good control over complex chemistries, and the opportunity for high-throughput experimentation. Other direct liquid-to-solid precursors exist, and have been shown to achieve complex honeycomb architectures; the discussion is limited here to easily implementable methods [75]. However, several wet-chemical techniques are relatively new in the ceramics field and require exploration of their potential for use in high-throughput materials research. Four common wet-chemical processing methods, sequential decomposition synthesis, dip coating, spin coating, and inkjet printing, are compared considering their adaptability for high-throughput synthesis in Figure 4, where we indicate scalability, automation considerations, and general advantages and disadvantages.

Sequential decomposition synthesis (Figure 4) is a direct liquid precursor-to-solid film route based on classic spray pyrolysis followed by low-temperature annealing to yield dense and crack-free films without classic sintering [76]. For example, it has been demonstrated to achieve a thick ceramic film (~10 μm) of $Li_7La_3Zr_2O_{12}$ (LLZO) by annealing at only 750°C [72]. Here, a precursor solution is atomized through a spray head or other dispersion tool onto a heated substrate where the dissolved precursor salts decompose via multiple pyrolysis reactions directly into a dense film at various rates (e.g. ~10 μm h^{-1}). The film microstructure (thickness, grain size, and porosity) can be tuned by controlling the spray solution composition, injection rate of solution into the spray head, dispensed volume, and deposition temperature [77]. Its potential for high throughput is strong because multiple precursor solutions can be simultaneously injected into the spray head to rapidly adjust film stoichiometries. Besides, semi-automation of the following components has been achieved in the past: (i) solution flow rate and dispensed volume control via programmable syringe pumps [78], (ii) spray head x-y movement control [79], and (iii) digital temperature control [80]. Automated spraying of solutions has been achieved in the automotive industry and, as such, we judge this technique to be the most promising synthetic method for high-throughput experimental campaigns.

Dip-coating (Figure 4) is based on sol-gel chemistry [81] where a substrate is immersed in a precursor solution and then withdrawn under controlled conditions [82] at a chosen rate (e.g., 10 μm h^{-1}) [83]. The coating thickness is defined by the withdrawal speed, precursor concentration, and viscosity [81]. Sequential dip-coating units that automatically cycle between multiple dipping solutions [84, 85], and combinatorial dip-coating with a continuous or stepped film thickness gradient have been achieved [86, 87]. Dip coating requires inexpensive equipment and deposits films on the order of minutes, but offers little control over layer thickness feature precision. Automated dip coating has been used to make sensors and solid oxide fuel cell layers and has successfully became a standard in the biomedical industry for sterile coatings. This method has been used to fabricate Li-garnet solid-state electrolytes [88].

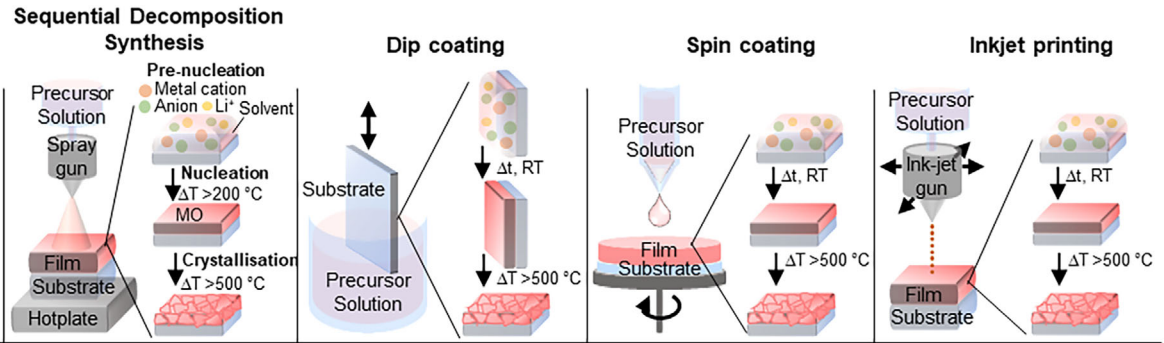

	Sequential Decomposition Synthesis	Dip coating	Spin coating	Inkjet printing
Scalability	Scale-up easy: moving spray nozzle, multiple spray heads	Continuous deposition, limited by drying	Limited by rotating stage size	Scale-up easy: moving inkjet print head
Automation maturity	Automated setup not commercially available	Simple automated setups available	Large-scale automated setups available	Automated setups available, but expensive
Automation potential in industry	Automotive industry: depositing paints	Nanomaterials and functional layers: SOFC Biomedical: coatings	Microelectronics: polymer films, magnetic storage discs Semiconductor: thin films	Office: printing on paper
Advantages	• Low cost • Good thickness, grain size, and porosity control • Easy deposition of full device stacks	• Low cost • Fast deposition times: minutes • Small space footprint	• Low cost • Fast deposition times: minutes • Small space footprint	• Fast deposition times: minutes to hours • Structure small features quickly • Easy deposition of full device stacks
Disadvantages	• Precursor formulations relatively new • Long depositions times: hours • Large space footprint	• Relatively low thickness ranges • Layers deposited on both sides of substrate • Requires sintering	• Relatively low thickness ranges • Easy stack deposition, poor layer shape control • Requires sintering	• High cost • Large space footprint • Limited inks available • Requires sintering

FIGURE 4 | Assessment of automation potential and integration into an automated closed-loop system of solid-state electrolyte synthesis techniques and structural characterization techniques. Solution-based fabrication techniques: sequential decomposition synthesis (SDS), dip-coating, spin-coating, ink-jet printing, and evaluation of their relative advantages and disadvantages, considering key criteria: scalability and automation maturity. MO, metal oxide; SOFC, solid oxide fuel cell.

Spin coating (Figure 4) is similar to dip coating in that it is also based on sol-gel chemistry, where the film is deposited through precipitation of a precursor solution onto a rotating substrate [81]. Key parameters for this technique include controlling film morphology and thickness by control of the angular velocity of the substrate, viscosity of precursor, and deposition time [89] of ~1 μm h^{-1} [90]. Spin coating has similar advantages and drawbacks to dip coating [91]. Spin coating is relatively autonomously mature and sees regular use in the semiconductor industry using 300 mm wafers to deposit polymer films. This method has been proposed for oxide solid-state electrolytes in batteries [92].

Ink-jet printing (Figure 4) is accomplished by voltage-controlled piezoelectric actuators expelling small droplets of ink from a well onto a substrate, followed by solvent evaporation and, potentially, annealing. Parameters that influence morphology are similar to those for spray pyrolysis-based techniques. Solution compatibility is a limiting factor: droplet size must be in the range of 10-100 pL [93], which varies with ink density, surface tension, and viscosity [94, 95]. Ink-jet printing offers ease of full device integration, scalability, good feature resolution [96], and high deposition speed [97–99]; however equipment can be relatively costly. Previously, automated printing of ceramic parts has been achieved for alumina materials [100], and mounting the printing head on a an x-y movable stage enabled printing on large areas [101]. This technique is industrially relevant as demonstrated by home and office printers. To the best of our knowledge, this method has not been used to make materials for batteries.

Current limitations of direct liquid precursor-to-solid film methods include (i) precursor solution determination, (ii) the complexity of multi-cation reactions, and (ii) a large design space, where many processing parameters influence resulting films. Precursor solutions must be crafted using metallic salts that have high solubility in organic solvents, and the aggregate boiling point must be low enough to be readily achievable at the lab benchtop. Parameter cross-coupling often leads to time-consuming exploration and difficulty in correlating processing-structure-property-performance relationships. Most oxide-based solid-state electrolytes are composed of at least two to four cations, and specific phases are required to ensure fast Li-ion conductivity. For example, for the deposition of Li-garnet (LLZO), multiple metal salt decomposition temperatures need to be coordinated with selection of solvents' respective boiling points, directed to achieve low deposition temperatures to control synthesis reactions and phase formations [102–104]. Another challenge is the drying and densification of the film, achieving a crack-free oxide film formation during chemical decomposition or pyrolysis reaction at deposition and post-annealing conditions [105], further complicated by a large variety of possible Li salts with

a wide range of thermal decomposition temperatures between 100–550°C. Densification is further impeded by an amorphous to polycrystalline phase transition and large resulting volume loss, leading to high stresses in the film. While these drawbacks are worth mentioning, it is possible to overcome them using the methods discussed in Section 3.1. Direct liquid precursor-to-solid film methods have the greatest potential for high-throughput experimental campaigns because they are faster in deposition and more easily automated, while allowing for rapid screening of high cation numbers than via solid-state synthesis.

5 | Perspective on Challenges and Advantages in High-Throughput Synthesis of Ceramic Materials

Typical deep learning uses at least tens of thousands of data points and even scales to millions or billions, depending on the application scenario; in contrast, ceramics fabrication produces samples several orders of magnitude slower, even when high-throughput synthesis methods are employed, thus requiring sophisticated computer-guided sample selection. In comparison to materials research, the pharmaceutical industry has been developing high-throughput systems for nearly 40 years because its products have a higher market value. For example, Ozempic earned Novo Nordisk 26 billion USD in 2024 [106]. In practice, pharmaceutical companies are willing to invest in high-throughput endeavors, whereas investment in ceramic material optimization and discovery is usually reserved for the capital required in companies to scale up components for device manufacturing, and its potential is not really achieved [107]. On the other hand, the renewable energy storage and conversion field, like the pharmaceutical industry before it, can benefit from high-throughput strategies to accelerate optimization, exploration, and exploitation of new materials. Through this work, we raise awareness that traditional ceramic synthesis must be re-examined using methods that are well-suited for high throughput, even if the methods being replaced are current industrial standards. For instance, the current ceramics research pipeline of mixing powders, calcining, pressing, and sintering to achieve a pellet or a tape is too slow and is unfit to realize the technological innovations by the time that industry and society requires them. Furthermore, using computer-aided decision making, the entire design space does not need to be explored and can instead be selectively sampled for new ceramic compounds, assisted by a smart high-throughput synthesis route of ceramic chemistries and compounds. This optimization saves resources, time, and effort and is one that the ceramics field should employ more frequently.

To make this shift, the most cost-effective and rapid synthesis methods should be used for ceramic components that allow changing chemistries and densification strategies at various levels. This regime change shifts away from past research goals of simple "cook and look" strategies aimed at narrow research questions or scale up to larger quantities of components by powder making and sintering. Specifically, we posit that direct liquid precursor-to-solid film methods are the most appropriate to be scaled up due to the film's inherent density and opportunity to synthesize complex phases incorporating several cations. In addition, high-information density characterization methods can increase the speed of material and device development. Finally, the precursor solutions can be readily adjusted to tailor the chemistry of the deposited film including precursor salt concentration, precursor identity, solvent identity, and stoichiometry. Concerning the battery industry, we see opportunities to rapidly discover novel electrolyte and electrode chemistries as well as to improve their industrial utility. The framework proposed here can lead to a new era of materials research just in time for a society that needs it.

Author Contributions

J.L.M.R., J.J.H., and K.P.S. conceived the concept of the perspective. J.J.H. and K.P.S. contributed to figure preparation. J.J.H. contributed to the structure design, research, figure preparation, discussion of the data, and writing of the manuscript. T.P., M.J.F., Y.T., E.O., and W.M. contributed to "data-guided methods". P.S. contributed to the materials synthesis and characterization methods. K.J.K. and J.L.J.M. contributed to the overall perspective of this article. J.L.M.R. supervised the work.

Acknowledgements

J.J.H. gratefully acknowledges support from the MIT Energy Initiative offered by ExxonMobil. This material is based upon work supported by the National Science Foundation Graduate Research Fellowship Program under Grant Number. 2141064. J.L.M.R. was financially supported by e-conversion, a Cluster of Excellence funded by the Deutsche Forschungsgemeinschaft (DFG, German Research Foundation). J.L.M.R., J.J.H. and T.P. wish to express their sincere gratitude to the Bavarian Ministry of Economic Affairs, Regional Development and Energy and TUMint.Energy Research GmbH for their generous support.

Open access funding enabled and organized by Projekt DEAL.

Funding

J.J.H. gratefully acknowledges support from the MIT Energy Initiative offered by ExxonMobil. This material is based upon work supported by the National Science Foundation Graduate Research Fellowship Program under Grant No. 2141064. J.L.M.R. was financially supported by e-conversion, a Cluster of Excellence funded by the Deutsche Forschungsgemeinschaft (DFG, German Research Foundation). J.L.M.R., J.J.H., and T.P. wish to express their sincere gratitude to the Bavarian Ministry of Economic Affairs, Regional Development and Energy and TUMint.Energy Research GmbH for their generous support.

Conflicts of Interest

The authors declare no conflicts of interest.

Data Availability Statement

The authors have nothing to report.

References

1. International Energy Outlook 2023 - U.S. Energy Information Administration (EIA) (2025).

2. J. Asenbauer, T. Eisenmann, M. Kuenzel, A. Kazzazi, Z. Chen, and D. Bresser, "The Success Story of Graphite as a Lithium-ion Anode Material—fundamentals, Remaining Challenges, and Recent Developments Including Silicon (oxide) Composites," *Sustainable Energy & Fuels* 4, no. 11 (2020): 5387–5416, https://doi.org/10.1039/D0SE00175A.

3. B. Tiede, C. O'Meara, and R. Jansen, "Battery Key Performance Projections Based on Historical Trends and Chemistries," *IEEE Transp Electrif Conf Expo* (2022): 754–759.

4. S. Sand, J. L. M. Rupp, and B. Yildiz, "A Critical Review on Li-Ion Transport, Chemistry And Structure Of Ceramic–Polymer Composite Electrolytes For Solid State Batteries," *Chemical Society Reviews* 54, no. 1 (2025): 178–200, https://doi.org/10.1039/D4CS00214H.

5. M. Balaish, K. J. Kim, H. Chu, et al., "Emerging Processing Guidelines for Solid Electrolytes in the Era of Oxide-based Solid-state Batteries," *Chemical Society Reviews* 54, no. 19 (2025): 8925–9007, https://doi.org/10.1039/D5CS00358J.

6. K. J. Kim, M. Balaish, M. Wadaguchi, L. Kong, and J. L. M. Rupp, "Solid-State Li–Metal Batteries: Challenges and Horizons of Oxide and Sulfide Solid Electrolytes and Their Interfaces," *Advanced Energy Materials* 11, no. 1 (2020): 2002689, https://doi.org/10.1002/aenm.202002689.

7. J. Janek and W. G. Zeier, "A Solid Future for Battery Development," *Nature Energy* 1 (2016): 1–4, https://doi.org/10.1038/nenergy.2016.141.

8. Y.-G. G. Lee, S. Fujiki, C. Jung, et al., "High-energy Long-cycling all-solid-state Lithium Metal Batteries Enabled by Silver–carbon Composite Anodes," *Nature Energy* 5 (2020): 299–308, https://doi.org/10.1038/s41560-020-0575-z.

9. R. Murugan, V. Thangadurai, and W. Weppner, "Fast Lithium Ion Conduction in Garnet-Type $Li_7La_3Zr_2O_{12}$," *Angewandte Chemie International Edition* 46, no. 41 (2007): 7778–7781, https://doi.org/10.1002/anie.200701144.

10. A. Ramzy and V. Thangadurai, "Tailor-Made Development of Fast Li Ion Conducting Garnet-Like Solid Electrolytes," *ACS Applied Materials & Interfaces* 2, no. 2 (2010): 385–390, https://doi.org/10.1021/am900643t.

11. Y. X. Gao, X. P. Wang, W. G. Wang, Z. Zhuang, D. M. Zhang, and Q. F. Fang, "Synthesis, Ionic Conductivity, and Chemical Compatibility of Garnet-Like Lithium Ionic Conductor $Li_5La_3Bi_2O_{12}$," *Solid State Ionics* 181, no. 31 (2010): 1415–1419, https://doi.org/10.1016/j.ssi.2010.08.012.

12. M. S. Beal, B. E. Hayden, T. Le Gall, et al., "High Throughput Methodology for Synthesis, Screening, and Optimization of Solid state Lithium Ion Electrolytes," *ACS Combinatorial Science* 13 (2011): 375–381, https://doi.org/10.1021/co100075f.

13. A. D. Spong, G. Vitins, S. Guerin, B. E. Hayden, A. E. Russell, and J. R. Owen, "Combinatorial Arrays and Parallel Screening for Positive Electrode Discovery," *Journal of Power Sources* 119-121 (2003): 778–783, https://doi.org/10.1016/S0378-7753(03)00252-0.

14. G. Ceder, "Opportunities and Challenges for First-principles Materials Design and Applications to Li Battery Materials," *MRS Bulletin* 35 (2010): 693–701, https://doi.org/10.1557/mrs2010.681.

15. S. Kirklin, B. Meredig, and C. Wolverton, "High-Throughput Computational Screening of New Li-Ion Battery Anode Materials," *Advanced Energy Materials* 3 (2013): 252–262, https://doi.org/10.1002/aenm.201200593.

16. W. D. Richards, L. J. Miara, Y. Wang, J. C. Kim, and G. Ceder, "Interface Stability in Solid-State Batteries," *Chemistry of Materials* 28 (2016): 266–273, https://doi.org/10.1021/acs.chemmater.5b04082.

17. Z. Ahmad, T. Xie, C. Maheshwari, J. C. Grossman, and V. Viswanathan, "Machine Learning Enabled Computational Screening of Inorganic Solid Electrolytes for Suppression of Dendrite Formation in Lithium Metal Anodes," *ACS Central Science* 4 (2018): 996–1006, https://doi.org/10.1021/acscentsci.8b00229.

18. L. Kahle, A. Marcolongo, and N. Marzari, "High-throughput Computational Screening for Solid-state Li-ion Conductors," *Energy & Environmental Science* 13 (2020): 928–948, https://doi.org/10.1039/C9EE02457C.

19. R. Mahbub, K. Huang, Z. Jensen, Z. D. Hood, J. L. M. Rupp, and E. A. Olivetti, "Text Mining for Processing Conditions of Solid-State Battery Electrolytes," *Electrochemistry Communications* 121 (2020): 106860, https://doi.org/10.1016/j.elecom.2020.106860.

20. A. Baliyan and H. Imai, "Machine Learning Based Analytical Framework for Automatic Hyperspectral Raman Analysis of Lithium-ion Battery Electrodes," *Scientific Reports* 9 (2019): 18241, https://doi.org/10.1038/s41598-019-54770-2.

21. J. Liu and F. Ciucci, "The Gaussian Process Distribution of Relaxation Times: A Machine Learning Tool for the Analysis and Prediction of Electrochemical Impedance Spectroscopy Data," *Electrochimica Acta* 331 (2020): 135316, https://doi.org/10.1016/j.electacta.2019.135316.

22. A. Nuhic, T. Terzimehic, T. Soczka-Guth, M. Buchholz, and K. Dietmayer, "Health Diagnosis and Remaining Useful Life Prognostics of Lithium-ion Batteries Using Data-driven Methods," *Journal of Power Sources* 239 (2013): 680–688, https://doi.org/10.1016/j.jpowsour.2012.11.146.

23. K. A. Severson, P. M. Attia, N. Jin, et al., "Data-driven Prediction of Battery Cycle Life Before Capacity Degradation," *Nature Energy* 4 (2019): 383–391, https://doi.org/10.1038/s41560-019-0356-8.

24. S. Shen, M. Sadoughi, M. Li, Z. Wang, and C. Hu, "Deep Convolutional Neural Networks With Ensemble Learning and Transfer Learning for Capacity Estimation of Lithium-ion Batteries," *Applied Energy* 260 (2020): 114296, https://doi.org/10.1016/j.apenergy.2019.114296.

25. N. J. Szymanski, B. Rendy, Y. Fei, et al., "An Autonomous Laboratory for the Accelerated Synthesis of Inorganic Materials," *Nature* 624, no. 7990 (2023): 86–91, https://doi.org/10.1038/s41586-023-06734-w.

26. M. Balaish, J. C. Gonzalez-Rosillo, K. J. Kim, Y. Zhu, Z. D. Hood, and J. L. M. Rupp, "Processing Thin but Robust Electrolytes for Solid-state Batteries," *Nature Energy* 6, no. 3 (2021): 227–239, https://doi.org/10.1038/s41560-020-00759-5.

27. D. Xue, P. V. Balachandran, J. Hogden, J. Theiler, D. Xue, and T. Lookman, "Accelerated Search for Materials With Targeted Properties by Adaptive Design," *Nature Communications* 7 (2016): 1–9, https://doi.org/10.1038/ncomms11241.

28. B. Sanchez-Lengeling and A. Aspuru-Guzik, "Inverse Molecular Design Using Machine Learning: Generative Models for Matter Engineering," *Science* 361 (2018): 360–365, https://doi.org/10.1126/science.aat2663.

29. P. J. Larkin, *Infrared and Raman Spectroscopy: Principles and Spectral Interpretation* (2017).

30. Q. Liang, S. Dwaraknath, and K. A. Persson, "High-throughput Computation and Evaluation of Raman Spectra," *Scientific Data* 6 (2019): 135, https://doi.org/10.1038/s41597-019-0138-y.

31. J. Liu, M. Osadchy, L. Ashton, M. Foster, C. J. Solomon, and S. J. Gibson, "Deep Convolutional Neural Networks for Raman Spectrum Recognition: A Unified Solution," *The Analyst* 142 (2017): 4067–4074, https://doi.org/10.1039/C7AN01371J.

32. T. Thompson, J. Wolfenstine, J. L. Allen, et al., "Tetragonal vs. Cubic Phase Stability in Al—Free Ta Doped $Li_7La_3Zr_2O_{12}$ (LLZO)," *Journal of Materials Chemistry A* 2, no. 33 (2014): 13431–13436, https://doi.org/10.1039/C4TA02099E.

33. H. S. Stein, "Combinatorial Synthesis and High-Throughput Investigation of Thin-Film Photocathodes and Catalysts for Solar Water Splitting," (2017).

34. S. Weinmann, H. Gobena, L. Quincke, et al., "Stabilizing Interfaces of All-Ceramic Composite Cathodes for Li-Garnet Batteries (Adv. Energy Mater. 37/2025)," *Advanced Energy Materials* 15, no. 37 (2025): 70184, https://doi.org/10.1002/aenm.70184.

35. C. Roitzheim, Y. J. Sohn, L.-Y. Kuo, et al., "All-Solid-State Li Batteries With NCM–Garnet-Based Composite Cathodes: The Impact of NCM Composition on Material Compatibility," *ACS Applied Energy Materials* 5, no. 6 (2022): 6913–6926, https://doi.org/10.1021/acsaem.2c00533.

36. Y. Xiao, L. J. Miara, Y. Wang, and G. Ceder, "Computational Screening of Cathode Coatings for Solid-State Batteries," *Joule* 3, no. 5 (2019): 1252–1275, https://doi.org/10.1016/j.joule.2019.02.006.

37. S. Randau, D. A. Weber, O. Kötz, et al., "Benchmarking the Performance of All-Solid-State Lithium Batteries," *Nature Energy* 5 (2020): 259–270, https://doi.org/10.1038/s41560-020-0565-1.

38. F. Flatscher, M. Philipp, S. Ganschow, H. M. R. Wilkening, and D. Rettenwander, "The Natural Critical Current Density Limit for

$Li_7La_3Zr_2O_{12}$ Garnets," *Journal of Materials Chemistry A* 8 (2020): 15782–15788, https://doi.org/10.1039/C9TA14177D.

39. Y. Xing, W. He, M. Pecht, and K. L. Tsui, "State of Charge Estimation of Lithium-ion Batteries Using the Open-circuit Voltage at Various Ambient Temperatures," *Applied Energy* 113 (2014): 106–115, https://doi.org/10.1016/j.apenergy.2013.07.008.

40. H. Pan, Z. Lü, W. Lin, J. Li, and L. Chen, "State of Charge Estimation of Lithium-ion Batteries Using a Grey Extended Kalman Filter and a Novel Open-circuit Voltage Model," *Energy* 138 (2017): 764–775, https://doi.org/10.1016/j.energy.2017.07.099.

41. W. Wang, N. W. Brady, C. Liao, et al., "High-Fidelity State-of-Charge Estimation of Li-Ion Batteries Using Machine Learning," (2019): 1–8, https://arxiv.org/abs/1909.02448.

42. A. J. Bard and L. R. Faulkner, *Electrochemical Methods: Fundamentals and Applications* (Wiley, 2000).

43. L. Wu, X. Fu, and Y. Guan, "Review of the Remaining Useful Life Prognostics of Vehicle Lithium-ion Batteries Using Data-driven Methodologies," *Applied Sciences* 6 (2016): 166, https://doi.org/10.3390/app6060166.

44. C. S. Chin and Z. Gao, "State-of-charge Estimation of Battery Pack Under Varying Ambient Temperature Using an Adaptive Sequential Extreme Learning Machine," *Energies* 11 (2018): 711, https://doi.org/10.3390/en11040711.

45. S. Curtarolo, G. L. W. Hart, M. B. Nardelli, N. Mingo, S. Sanvito, and O. Levy, "The High-throughput Highway to Computational Materials Design," *Nature Materials* 12 (2013): 191–201, https://doi.org/10.1038/nmat3568.

46. P. M. Attia, A. Grover, N. Jin, et al., "Closed-loop Optimization of Fast-charging Protocols for Batteries With Machine Learning," *Nature* 578, no. 7795 (2020): 397–402, https://doi.org/10.1038/s41586-020-1994-5.

47. P. Ma, T. Du, and W. Matusik, Efficient Continuous Pareto Exploration in Multi-Task Learning Proceedings of the 37th International Conference on Machine Learning, PMLR 119 (2020): 6522–6531.

48. A. Jain, S. P. Ong, G. Hautier, et al., "Commentary: The Materials Project: A Materials Genome Approach to Accelerating Materials Innovation," *APL Materials* 1, no. 1 (2013): 11002, https://doi.org/10.1063/1.4812323.

49. R. A. Fisher, *The Design of Experiments* (Oliver & Boyd, 1935).

50. Q. Liang, A. E. Gongora, Z. Ren, et al., "Benchmarking the Performance of Bayesian Optimization Across Multiple Experimental Materials Science Domains," *npj Computational Materials* 7, no. 1 (2021): 188, https://doi.org/10.1038/s41524-021-00656-9.

51. P. I. Frazier and J. Wang, "Bayesian Optimization for Materials Design," in *Information Science for Materials Discovery and Design*, ed. T. Lookman, F. J. Alexander, and K. Rajan, (Springer International Publishing, 2016), 45–75.

52. B. Shahriari, K. Swersky, Z. Wang, R. P. Adams, and N. Freitas, "Taking the Human out of the Loop: A Review of Bayesian Optimization," *Proceedings of the IEEE* 104, no. 1 (2016): 148–175, https://doi.org/10.1109/JPROC.2015.2494218.

53. T. Erps, M. Foshey, M. K. Luković, et al., "Accelerated Discovery of 3D Printing Materials Using Data-driven Multiobjective Optimization," *Science Advances* 7, no. 42 (2022): abf7435, https://doi.org/10.1126/sciadv.abf7435.

54. A. Dave, J. Mitchell, K. Kandasamy, et al., "Autonomous Discovery of Battery Electrolytes With Robotic Experimentation and Machine Learning," *Cell Reports Physical Science* 1, no. 12 (2020): 100264, https://doi.org/10.1016/j.xcrp.2020.100264.

55. R. Moriconi, M. P. Deisenroth, and S. Kumar, "High-dimensional Bayesian Optimization Using Low-dimensional Feature Spaces," *Machine learning* 109, no. 9 (2020): 1925–1943, https://doi.org/10.1007/s10994-020-05899-z.

56. A. Benayad, D. Diddens, A. Heuer, et al., "High-Throughput Experimentation and Computational Freeway Lanes for Accelerated Battery Electrolyte and Interface Development Research," *Advanced Energy Materials* 12, no. 17 (2022): 2102678, https://doi.org/10.1002/aenm.202102678.

57. A. Dave, J. Mitchell, S. Burke, H. Lin, J. Whitacre, and V. Viswanathan, "Autonomous Optimization of Non-aqueous Li-ion Battery Electrolytes via Robotic Experimentation and Machine Learning Coupling," *Nature Communications* 13, no. 1 (2022): 5454, https://doi.org/10.1038/s41467-022-32938-1.

58. C. Karpovich, E. Pan, Z. Jensen, and E. Olivetti, "Interpretable Machine Learning Enabled Inorganic Reaction Classification and Synthesis Condition Prediction," *Chemistry of Materials* 35, no. 3 (2023): 1062–1079, https://doi.org/10.1021/acs.chemmater.2c03010.

59. H. Huo, Z. Rong, O. Kononova, et al., "Semi-supervised Machine-learning Classification of Materials Synthesis Procedures," *Npj Computational Materials* 5, no. 1 (2019): 62.

60. E. Kim, K. Huang, A. Saunders, A. McCallum, G. Ceder, and E. Olivetti, "Materials Synthesis Insights From Scientific Literature via Text Extraction and Machine Learning," *Chemistry of Materials* 29, no. 21 (2017): 9436–9444, https://doi.org/10.1021/acs.chemmater.7b03500.

61. O. Kononova, H. Huo, T. He, et al., "Text-mined Dataset of Inorganic Materials Synthesis Recipes," *Scientific Data* 6, no. 1 (2019): 203, https://doi.org/10.1038/s41597-019-0224-1.

62. H. Huo, C. J. Bartel, T. He, et al., "Machine-Learning Rationalization and Prediction of Solid-State Synthesis Conditions," *Chemistry of Materials* 34, no. 16 (2022): 7323–7336, https://doi.org/10.1021/acs.chemmater.2c01293.

63. T. Prein, E. Pan, J. Jehkul, S. Weinmann, E. Olivetti, and J. L. M. Rupp, "Language Models Enable Data-Augmented Synthesis Planning for Inorganic Materials," *ACS Applied Materials & Interfaces* 17, no. 51 (2025): 69221–69233, https://doi.org/10.1021/acsami.5c11229.

64. Z. Wang, O. Kononova, K. Cruse, et al., "Dataset of Solution-based Inorganic Materials Synthesis Procedures Extracted From the Scientific Literature," *Scientific Data* 9, no. 1 (2022): 231, https://doi.org/10.1038/s41597-022-01317-2.

65. T. Prein, E. Pan, S. Haddouti, et al., Retro-Rank-In: A Ranking-Based Approach for Inorganic Materials Synthesis Planning (2025), https://arxiv.org/abs/2502.04289.

66. T. Prein, F. Rahmanian, K. P. Arul, et al., "Reaction Graph Networks for Inorganic Synthesis Condition Prediction of Solid State Materials," *AI Accel Mater Des—NeurIPS* (2024).

67. X. Jia, A. Lynch, Y. Huang, et al., "Anthropogenic Biases in Chemical Reaction Data Hinder Exploratory Inorganic Synthesis," *Nature* 573, no. 7773 (2019): 251–255, https://doi.org/10.1038/s41586-019-1540-5.

68. O. Kononova, T. He, H. Huo, A. Trewartha, E. A. Olivetti, and G. Ceder, "Opportunities and Challenges of Text Mining in Materials Research," *iScience* 24, no. 3 (2021): 102155, https://doi.org/10.1016/j.isci.2021.102155.

69. X. Wei, X. Cui, N. Cheng, et al., "ChatIE: Zero-Shot Information Extraction via Chatting with ChatGPT," Zero-Shot Information Extraction via Chatting with ChatGPT, (2023), https://arxiv.org/abs/2302.10205.

70. S. A. Malik, R. E. A. Goodall, and A. A. Lee, "Predicting the Outcomes of Material Syntheses With Deep Learning," *Chemistry of Materials* 33, no. 2 (2021): 616–624, https://doi.org/10.1021/acs.chemmater.0c03885.

71. D. P. Kingma and M. Welling, "Auto-Encoding Variational Bayes," (2022), https://arxiv.org/abs/1312.6114.

72. Z. D. Hood, Y. Zhu, L. J. Miara, W. S. Chang, P. Simons, and J. L. M. Rupp, "A Sinter-free Future for Solid-state Battery Designs," *Energy & Environmental Science* 15, no. 7 (2022): 2927–2936, https://doi.org/10.1039/D2EE00279E.

73. R. Pfenninger, M. Struzik, I. I. Garbayo, E. Stilp, and J. L. Rupp, "A low ride on processing temperature for fast lithium conduction in garnet

solid-state battery films," *Nature Energy* 4, no. 6 (2019): 475–483, https://doi.org/10.1038/s41560-019-0384-4.

74. A. Czapla and E. Kusior, "Mixed oxide Al-Ti films obtained by sputtering of a segmented target," *Physica Status Solidi (a)* 140, no. 2 (1993): K81–K84, https://doi.org/10.1002/pssa.2211400236.

75. J. Bu, P. Leung, C. Huang, S. H. Lee, and P. S. Grant, "Co-spray Printing of $LiFePO_4$ and PEO-$Li_{1.5}Al_{0.5}Ge_{1.5}(PO_4)_3$ Hybrid Electrodes for All-Solid-State Li-ion Battery Applications," *Journal of Materials Chemistry A* 7, no. 32 (2019): 19094–19103, https://doi.org/10.1039/C9TA03824H.

76. J. L. M. Rupp, B. Scherrer, and L. J. Gauckler, "Engineering Disorder in Precipitation-based Nano-scaled Metal Oxide Thin Films," *Physical Chemistry Chemical Physics* 12, no. 36 (2010): 11114–11124, https://doi.org/10.1039/b920971a.

77. L. Filipovic, S. Selberherr, G. C. Mutinati, et al., "Modeling Spray Pyrolysis Deposition," *Proceedings of the World Congress on Engineering* 2 (2013): 987–992.

78. M. V. Santhosh, C. S. Kartha, and K. P. Vijayakumar, "Improvement of Device Parameters of $CuInS_2/In_2S_3$ Junction Deposited Using Automated Spray Machine," *Aip Conference Proceedings* 1349 (2011): 673–674, https://doi.org/10.1063/1.3606037.

79. V. G. Krishnan, P. Elango, V. Ganesan, and P. Sathish, "pH Deeds on Structural, Optical, Electrical and Gas Sensing Performance of TiO_2 Nanofilms by Automated Nebulizer Spray Pyrolysis Technique," *Optik* 127 (2016): 11102–11110, https://doi.org/10.1016/j.ijleo.2016.09.032.

80. K. Ravichandran, N. Dineshbabu, T. Arun, A. Manivasaham, and E. Sindhuja, "Synergistic Effects of Mo and F Doping on the Quality Factor of ZnO Thin Films Prepared by a Fully Automated Home-made Nebulizer Spray Technique," *Applied Surface Science* 392 (2017): 624–633, https://doi.org/10.1016/j.apsusc.2016.09.079.

81. C. J. Brinker, A. J. Hurd, P. R. Schunk, G. C. Frye, and C. S. Ashley, "Review of Sol-gel Thin Film Formation," *Journal of Non-Crystalline Solids* 147-148 (1992): 424–436, https://doi.org/10.1016/S0022-3093(05)80653-2.

82. Y. Lu, R. Ganguli, C. A. Drewien, et al., "Continuous Formation of Supported Cubic and Hexagonal Mesoporous Films by Sol–gel Dip-coating," *Nature* 389 (1997): 364–368, https://doi.org/10.1038/38699.

83. M. Niazmand, A. Maghsoudipour, M. Alizadeh, Z. Khakpour, and A. Kariminejad, "Effect of Dip Coating Parameters on Microstructure and Thickness of 8YSZ Electrolyte Coated on NiO-YSZ by Sol-gel Process for SOFCs Applications," *Ceramics International* 48, no. 11 (2022): 16091–16098, https://doi.org/10.1016/j.ceramint.2022.02.155.

84. M. Schneider, C. Günter, and A. Taubert, "Co-Deposition of a Hydrogel/Calcium Phosphate Hybrid Layer on 3D Printed Poly (Lactic Acid) Scaffolds via Dip Coating: Toward Automated Biomaterials Fabrication," *Polymers* 10 (2018): 275, https://doi.org/10.3390/polym10030275.

85. M. Adnan and J. K. Lee, "All Sequential Dip-Coating Processed Perovskite Layers From an Aqueous Lead Precursor for High Efficiency Perovskite Solar Cells," *Scientific Reports* 8 (2018): 2168, https://doi.org/10.1038/s41598-018-20296-2.

86. M. Faustini, D. R. Ceratti, B. Louis, M. Boudot, P. Albouy, and D. Grosso, "Engineering Functionality Gradients by Dip Coating Process in Acceleration Mode," *ACS Applied Materials & Interfaces* 6 (2014): 17102, https://doi.org/10.1021/am504770x.

87. K. Mokurala, L. L. Baranowski, F. W. D. S. Lucas, et al., "Combinatorial Chemical Bath Deposition of CdS Contacts for Chalcogenide Photovoltaics," *ACS Combinatorial Science* 18 (2016): 583, https://doi.org/10.1021/acscombsci.6b00074.

88. K. Tadanaga, H. Egawa, A. Hayashi, et al., "Preparation of Lithium Ion Conductive Al-doped $Li_7La_3Zr_2O_{12}$ Thin Films by a Sol–Gel Process," *Journal of Power Sources* 273 (2015): 844–847, https://doi.org/10.1016/j.jpowsour.2014.09.164.

89. D. E. Bornside, C. W. Macosko, and L. E. Scriven, "Spin Coating: One-dimensional Model," *Journal of Applied Physics* 66 (1989): 5185, https://doi.org/10.1063/1.343754.

90. M. Zarabian, M. Bartolini, P. Pereira-Almao, and V. Thangadurai, "X-ray Photoelectron Spectroscopy and AC Impedance Spectroscopy Studies of Li-La-Zr-O Solid Electrolyte Thin Film/LiCoO2 Cathode Interface for all-Solid-State Li Batteries," *Journal of The Electrochemical Society* 164 (2017): A1133–A1139, https://doi.org/10.1149/2.0621706jes.

91. C. J. Brinker, C. S. Ashley, and R. A. Cairncross, "Sol-gel Derived Ceramic Films — Fundamentals and applications," in *Metallurgical and Ceramic Protective Coatings* (1996), https://doi.org/10.1007/978-94-009-1501-5.

92. R. J. Chen, M. Huang, W. Z. Huang, Y. Shen, Y. H. Lin, and C. W. Nan, "Sol–gel derived Li–La–Zr–O thin films as solid electrolytes for lithium-ion batteries," *Journal of Materials Chemistry A* 2 (2014): 13277–13282, https://doi.org/10.1039/C4TA02289K.

93. B. Derby, "Additive Manufacture of Ceramics Components by," *Inkjet Printing Engineering* 1 (2015): 113–123.

94. J. Mei, M. R. Lovell, and M. H. Mickle, "Formulation and Processing of Novel Conductive Solution Inks in Continuous Inkjet Printing of 3-D Electric Circuits," *IEEE Transactions on Electronics Packaging Manufacturing* 28 (2005): 265–273.

95. A. Friederich, J. R. Binder, and W. Bauer, "Rheological Control of the Coffee Stain Effect for Inkjet Printing of Ceramics," *Journal of the American Ceramic Society* 96 (2013): 2093–2099, https://doi.org/10.1111/jace.12385.

96. J. Stringer and B. Derby, "Limits to Feature Size and Resolution in Ink Jet Printing," *Journal of the European Ceramic Society* 29 (2009): 913–918, https://doi.org/10.1016/j.jeurceramsoc.2008.07.016.

97. B. Cappi, E. Özkol, J. Ebert, and R. Telle, "Direct Inkjet Printing of Si3N4: Characterization of Ink, Green Bodies and Microstructure," *Journal of the European Ceramic Society* 28 (2008): 2625–2628, https://doi.org/10.1016/j.jeurceramsoc.2008.03.004.

98. J. H. Song and H. M. Nur, "Defects and Prevention in Ceramic Components Fabricated by Inkjet Printing," *Journal of Materials Processing Technology* 155-156 (2004): 1286–1292, https://doi.org/10.1016/j.jmatprotec.2004.04.292.

99. E. Özkol, J. Ebert, K. Uibel, A. M. Wätjen, and R. Telle, "Development of High Solid Content Aqueous 3Y-TZP Suspensions for Direct Inkjet Printing Using a Thermal Inkjet Printer," *Journal of the European Ceramic Society* 29 (2009): 403–409.

100. C. Ainsley, N. Reis, and B. Derby, "Freeform Fabrication by Controlled Droplet Deposition of Powder Filled Melts," *Journal of Materials Science* 37 (2002): 3155–3161, https://doi.org/10.1023/A:1016106311185.

101. J. Lim, J. Kim, Y. J. Yoon, et al., "All-Inkjet-Printed Metal-Insulator-Metal (MIM) Capacitor," *Current Applied Physics* 12 (2012): e14–e17, https://doi.org/10.1016/j.cap.2011.04.035.

102. R. Djenadic, M. Botros, C. Benel, et al., "Nebulized Spray Pyrolysis of Al-doped $Li_7La_3Zr_2O_{12}$ Solid Electrolyte for Battery Applications," *Solid State Ionics* 263 (2014): 49–56, https://doi.org/10.1016/j.ssi.2014.05.007.

103. J. Sakamoto, E. Rangasamy, H. Kim, Y. Kim, and J. Wolfenstine, "Synthesis of Nano-scale Fast Ion Conducting Cubic $Li_7La_3Zr_2O_{12}$," *Nanotechnology* 24 (2013): 424005, https://doi.org/10.1088/0957-4484/24/42/424005.

104. X. Han, Y. Gong, K. Fu, et al., "Negating Interfacial Impedance in Garnet-based Solid-state Li Metal Batteries," *Nature Materials* 16 (2017): 572–579, https://doi.org/10.1038/nmat4821.

105. M. Bitzer, T. Van Gestel, and S. Uhlenbruck, "Sol-gel Synthesis of Thin Solid $Li_7La_3Zr_2O_{12}$ Electrolyte Films for Li-ion Batteries," *Thin Solid Films* 615 (2016): 128–134, https://doi.org/10.1016/j.tsf.2016.07.010.

106. V. Walt, *Ozempic and Wegovy Pumped $26 Billion Into Novo Nordisk Last Year. Can the Pharma Giant Find Its next Breakthrough Before the*

Boom Ends? (Fortune, 2025), https://fortune.com/2025/03/31/ozempic-wegovy-novo-nordisk-nvidia/.

107. D. Chung, E. Elgqvist, and S. Santhanagopalan, "Automotive Lithium-ion Cell Manufacturing: Regional Cost Structures and Supply Chain Considerations," (2016), https://doi.org/10.2172/1247459.

Supporting Information

Additional supporting information can be found online in the Supporting Information section.

Supporting File: aenm70703-sup-0001-SuppMat.docx.